Research Square

Preprints are preliminary reports that have not undergone peer review.
They should not be considered conclusive, used to inform clinical practice,
or referenced by the media as validated information.

Increased Zoonotic Risk Posed by Emerging Haemagglutinin Variants of Clade 2.3.4.4b A(H5Nx) High Pathogenicity Avian Influenza Virus

Munir Iqbal

munir.iqbal@pirbright.ac.uk

The Pirbright Institute https://orcid.org/0000-0001-5165-5339

Jiayun Yang

The Pirbright Institute, Woking, Surrey, UK, GU24 0NF

Elizabeth Billington

Animal and Plant Health Agency

William Harvey

University of Edinburgh https://orcid.org/0000-0001-9529-1127

Sofia Riccio

Animal and Plant Health Agency

Simon Johnson

Animal and Plant Health Agency

Kristel Ramirez Valdez,

The Pirbright Institute, Woking, Surrey, UK, GU24 0NF

Hannah Klim

Department of Infectious Diseases, Imperial College London, UK, W2 1PG

Ksenia Sukhova

Imperial College London https://orcid.org/0000-0003-3678-5631

Jin Yu

Imperial College London

Thusitha Karunarathna

The Pirbright Institute

Mehnaz Qureshi

The Pirbright Institute

Samuel Richardson

The Pirbright Institute https://orcid.org/0000-0001-7149-3832

Toby Carter

The Pirbright Institute

Jafar Hassan

Animal and Plant Health Agency

Cecilia Genova
Animal and Plant Health Agency

Georgina Ward
Animal and Plant Health Agency

Kelly Roper
Animal and Plant Health Agency

Jean-Remy Sadeyen
The Pirbright Institute

Dorothy Hawkins
The Francis Crick Institute, London, UK

Tereza Masonou
Great Ormond Street UCL Institute of Child Health, London, UK https://orcid.org/0000-0003-3663-8965

Maximillian Woodall
University College London https://orcid.org/0000-0003-4511-9171

Claire Smith
University College London https://orcid.org/0000-0002-8913-0009

Yan Liu
Glycosciences Laboratory, Imperial College London https://orcid.org/0000-0002-2566-6867

Marek Slomka
Animal and Plant Health Agency

Ashley Banyard
Animal and Plant Health Agency https://orcid.org/0000-0002-1286-9825

Thomas Peacock
The Pirbright Institute https://orcid.org/0000-0001-7077-2928

Ian Brown
Pirbright Institute https://orcid.org/0000-0003-3909-1301

Paul Digard
University of Edinburgh https://orcid.org/0000-0002-0872-9440

Samantha Lycett
University of Edinburgh https://orcid.org/0000-0003-3159-596X

Wendy Barclay
Imperial College London https://orcid.org/0000-0002-3948-0895

Joe James
Animal and Plant Health Agency (APHA) https://orcid.org/0000-0002-9673-3684

Biological Sciences - Article

Keywords:

Posted Date: November 3rd, 2026

DOI: https://doi.org/10.21203/rs.3.rs-11578744/v1

License: This work is licensed under a Creative Commons Attribution 4.0 International License.
Read Full License

Additional Declarations: There is **NO** Competing Interest.

Increased Zoonotic Risk Posed by Emerging Haemagglutinin Variants of Clade 2.3.4.4b A(H5Nx) High Pathogenicity Avian Influenza Virus

Jiayun Yang[1*], Elizabeth Billington[2*], William T. Harvey[3], Sofia Riccio[2], Simon Johnson[2], Kristel Ramirez Valdez[1], Hannah Klim[4], Ksenia Sukhova[4], Jin Yu[5], Thusitha K. Karunarathna[1], Mehnaz Qureshi[1], Samuel A.S. Richardson[1], Toby Carter[1], Jafar Hassan[2], Cecilia Di Genova[2], Georgina Ward[2], Kelly Roper[2], Jean-Remy Sadeyen[1], Dorothy E.D.P. Hawkins[6], Tereza Masonou[7], Maximillian Woodall[7], Claire Smith[7], Yan Liu[5], Marek J. Slomka[2], Ashley C. Banyard[2,8], Thomas P. Peacock[1,4], Ian H. Brown[1, 2], Paul Digard[3], Samantha J. Lycett[3], Wendy S. Barclay[4], Joe James[2,4,8#], and Munir Iqbal[1#].

[1]The Pirbright Institute, Woking, UK
[2]Department of Virology, Animal and Plant Health Agency (APHA-Weybridge), Addlestone, UK
[3]The Roslin Institute, The University of Edinburgh, Easter Bush Campus, UK
[4]Department of Infectious Disease, Imperial College London, UK
[5]Glycosciences Laboratory, Department of Metabolism, Digestion and Reproduction, Faculty of Medicine, Imperial College London, London, UK
[6]The Francis Crick Institute, London, UK
[7]Great Ormond Street UCL Institute of Child Health, London, UK
[8]WOAH/FAO International Reference Laboratory for Avian Influenza, Animal and Plant Health Agency (APHA-Weybridge), Addlestone, UK
*Contributed equally
[#]Corresponding authors: Munir.iqbal@pirbright.ac.uk and Joe.james@apha.gov.uk

Abstract

High pathogenicity avian influenza viruses (HPAIVs) remain a major threat to animal and human health. The clade 2.3.4.4b H5Nx panzootic has been marked by increasing cross-species adaptation, including outbreaks in dairy cattle. The surge in mammalian infections in both wild and captive populations heighten concerns about zoonotic and pandemic potential. Here, we analyse haemagglutinin (HA) evolution in clade 2.3.4.4b H5Nx viruses from 2020 to 2025, focusing on key residues within the receptor-binding domain. We identify HA E185K (mature H5 HA numbering; E189K in H3 numbering) as a novel immune escape mutation that confers increased binding to avian- and human-type sialic acid receptors. Strikingly, this mutation is increasingly prevalent in cattle-derived H5N1 viruses and enhances binding to human-like receptors. However, ferret studies demonstrated that whilst pathogenicity of the E185K virus was comparable to the cattle derived isolate, the E185K mutation did not confer transmission to direct or indirect contact ferrets. Our results reveal a mechanism linking immune escape with expanded receptor specificity, highlighting a potential pathway for mammalian adaptation. These findings underscore the need for continued surveillance of evolving H5Nx viruses to mitigate emerging zoonotic threats.

Introduction

Avian influenza virus (AIV) infection is a major threat to wildlife, animal production, and public health worldwide. Since its first detection in 1996, the A/goose/Guangdong/1/1996 (H5N1) (gs/GD/96) lineage of high pathogenicity avian influenza (HPAI) H5 viruses has become epizootic globally[1,2]. This lineage has rapidly evolved into more than 30 clades and subclades, resulting in substantial antigenic diversity. Clade 2.3.4.4b emerged in 2016 and rapidly spread, driving the current global panzootic, with a notable shift from a previously dominant H5N8 subtype to the current circulating H5N1 subtype[3,4] occurring in 2020.

The clade 2.3.4.4b H5N1 virus has become the most dominant HPAI subtype, with apparent genomic plasticity resulting in substantial numbers of H5N1 genotypes being defined, causing unprecedented outbreaks in wild and domestic bird populations worldwide. While wild waterfowl remain important for clade 2.3.4.4b maintenance and dissemination, extensive reassortment has facilitated an expanded host range for some current H5N1 genotypes to include Charadriiformes (seabirds), establishing sustained lineages and resulting in altered disease ecologies[5-7]. Further, an expanded mammalian host range has been described through the detection of infection and mortalities in numerous mammalian species including, but not limited to, sea mammals, cats, minks and foxes[8-11]. In March 2024, clade 2.3.4.4b H5N1 was also detected in dairy cattle in the USA[12,13]. To date, H5N1 has been detected and reported in more than 21 states and over 1,000 confirmed outbreaks according to United States Department of Agriculture (https://www.aphis.usda.gov/livestock-poultry-disease/avian/avian-influenza/hpai-detections/hpai-confirmed-cases-livestock)). Human infections with the clade 2.3.4.4b H5N1 virus remain sporadic; 132 confirmed cases from 2020-2025 listed by the World Health Organization (WHO). Amongst these were 71 infections in the United States, 41 of which are associated with dairy farms. The sustained global circulation of this virus clade underscores the urgent need to assess its zoonotic spillover potential and associated risks to human health.

The binding specificity of the viral haemagglutinin (HA) protein to sialic acid (SA) containing glycans on cell surfaces is a key determinant of influenza virus host range. Influenza viruses of avian origin preferentially bind cell-surface glycans containing α2,3-linked sialic acids (SAα2,3Gal), whereas human seasonal and pandemic influenza viruses preferentially recognize α2,6-linked sialic acids (SAα2,6Gal)[14]. This specificity corresponds to the predominant distribution of α2,3-linked and α2,6-linked SA in the avian gastrointestinal tract and the human respiratory tract, respectively[15,16]. To overcome host barriers, AIVs frequently acquire adaptive mutations in HA that switch receptor-binding preference. In previous H5N1 HAs, substitutions such as T156A, Q222L and G224S have been shown to enhance binding to human-like SA[17-20],

thereby facilitating infection of mammalian hosts and potentially increasing the likelihood of onwards transmission.

The immunodominant HA protein also plays a central role in determining viral antigenicity and serves as the primary target of neutralizing antibodies. Consequently, HA evolution is often shaped by pre-existing immunity from vaccination or natural infection. Wild aquatic birds act as the natural reservoirs of low pathogenicity AIVs, in which the infection is typically established in the intestinal tract and is often associated with mild or asymptomatic disease. Recurrent infection and reinfection in these populations lead to the accumulation of post-infection immunity, which exerts sustained selective pressure on circulating viruses. High intensity vaccination of poultry represents an additional, potent driver of AIV HA evolution. Countries including China, Egypt, Mexico, and Vietnam have implemented mass H5 vaccination campaigns in poultry, while many others are considering adopting a similar strategy[21]. However, vaccination programmes whilst a key element of future control strategies, could influence viral glycoprotein evolution through emergence of immune escape variants, leading to a possible reduction in vaccine efficacy[22]. Consequently, should more widespread poultry vaccination be adopted globally, the importance of monitoring for possible antibody-driven viral evolution will become epidemiologically relevant for the emergence of novel AIV strains.

Here, we investigated whether naturally occurring genetic variation in the HA receptor-binding region of clade 2.3.4.4b H5Nx viruses can alter receptor binding profiles and antigenic recognition, and whether these changes pose zoonotic risk. We first analysed genetic polymorphisms in this region and used reverse genetics (RG) to assess their functional effects on receptor binding. We then studied whether immune pressure exerted by antisera could select HA variants with altered receptor-binding specificity and antigenic cross-reactivity. Finally, we used a ferret model to assess the pathogenesis and transmission of the identified HA variants. Together, the data demonstrated how immune-driven adaptation can simultaneously promote antigenic escape and impact upon receptor binding, with potential implications for zoonotic risk.

Results

Overview of receptor binding regions of Clade 2.3.4.4b HA.

To investigate how emerging evolutionary changes in HPAI H5N1 viruses may affect virus–host interactions, we examined the major structural regions of the HA receptor-binding pocket (***all the subsequent H5 HA amino acid positions described are mature H5 HA numbering***): the 130 loop (residues 125-138), 190 helix (residues 181-197), and 220 loop (residues 213-229) within the receptor binding site (RBS)[23] (Supplementary Figure S1). Further, to assess temporal

variation, we compared the amino acid (aa) identity of these three receptor binding domains by year, applying a 99% conservation threshold. Residues with conservation below this threshold were considered less conserved (Supplementary Figure S2).

A total of 18 mutations at non-conserved RBSs were identified at frequencies of 1% or higher: E126D, T127A, S128A, V131M, P136Q, P136S, Y137H, S181P, N183S, A184E, A184V, E185K, T188A, T188I, N189D, N189K, A214S and A214V. Naturally occurring viruses (wild type; WT) containing these mutations were identified for further analysis (Table 1). The selected 18 mutations are indicated in the HA structure (Figure 1A). We generated RG viruses carrying the monobasic HA cleavage site (CS) and its homologous NA, with laboratory-adapted A/Puerto Rico/8/1934 (PR8) internal genes. In addition to the 18 WT-like viruses, A/chicken/England/053052/2021 (H5N1) (Ck/ENG/52/21) was included as a control virus representing the background strain, which contained none of the 18 mutations described above. Together, this panel provides a representative set of naturally occurring clade 2.3.4.4b HA variants, enabling systematic evaluation of their functional and antigenic properties relative to the consensus virus Ck/ENG/52/21.

Table 1. Panel of RG viruses analysed by BLI in this study.

Strain name	Abbreviation	Receptor binding profiles of control viruses and H5 HA mutations (Relative to Ck/ENG/52/21)
A/England/195/2009 (H1N1)	ENG/195/09	6SLN binding
A/duck/Vietnam/OIE-2202/2012 (H5N1)	Dk/VNM/02/12	3SLN binding
A/Anhui/1/2013 (H7N9)	AH/1/13	3SLN and 6SLN binding
A/chicken/Egypt/RIMD12-3/2008 (H5N1)	Ck/EG/2-3/08	3SLN and 6SLN binding
A/chicken/England/053052/2021 (H5N1)	Ck/ENG/52/21	Consensus
A/herring_Gull/England/123277/2023 (H5N5)	Gull/ENG/77/23	E126D
A/cat/SD/24-038917-001-original/2024 (H5N1)	Cat/SD/01/24	T127A
A/goose/Sweden/SVA210301SZ0005/KN049802-IP11/2021 (H5N8)	Gs/SE/11/2021	S128A
A/California/151/2024(H5N1)	CA/51/24	V131M
A/chicken/Scotland/068270/2021 (H5N1)	Ck/SCO/70/21	P136Q
A/turkey/England/039352/2020 (H5N8)	Ty/ENG/52/20	P136S
A/white mink/Finland/UH-357-E1/2023	Mink/FIN/E1/23	Y137H
A/common teal/South Korea/W812/2021 (H5N1)	Teal/KR/12/21	S181P
A/striped skunk/PE/FAV-0089-1/2023 (H5N1)	Skunk/PE/9-1/23	N183S
A/whooper swan/Fukushima/0701B002/2021 (H5N8)	Swan/Fuku/02/21	A184E
A/pheasant/England/331075/2022 (H5N1)	Ph/ENG/75/22	A184V
A/long-tailed_skua/Scotland/22/2022 (H5N1)	Skua/SCO/22/22	E185K
A/ardea_cinerea/Spain/863-1_22VIR6312-5/2022 (H5N1)	Ardea/ES/2-5/22	T188A
A/chicken/Chiba/T50-23/2021(H5N8)	Ck/CHB/23/21	T188I
A/chicken/Aomori/TU9-4142/2021 (H5N1)	Ck/AMR/42/21	N189D
A/black vulture/Georgia/W22-722C/2022 (H5N1)	Vul/GA/2C/22	N189K
A/chicken/USA/24-031166-001/2024 (H5N1)	Ck/USA/01/24	A214S
A/canada Goose/ON/FAV-0056-4-2024/2024 (H5N1)	Gs/ON/24/24	A214V

HA mutation E185K shows increased binding to human-like receptor.

Synthetic sialylated avian-like receptor analogues α2,3-sialyllactosamine (3SLN) and human-like receptor analogue α2,6-sialyllactosamine (6SLN) were used to assess the receptor binding profiles of the selected H5 viruses by bio-layer interferometry (BLI). A panel of control RG viruses were used to test the receptor binding specificity to 3SLN and 6SLN, including: a human 2009 pandemic A/England/195/2009 (H1N1), referred to as ENG/195/09 (H1N1), which exclusively binds to 6SLN, an avian virus A/duck/Vietnam/OIE-2202/2012 (H5N1), referred to as Dk/VNM/02/12 (H5N1), which exclusively binds to 3SLN, and a known dual-binding virus A/Anhui/1/2013 (H7N9), referred to as AH/1/13 (H7N9), which binds to both 3SLN and 6SLN (Figure 1B-1D)[24-26]. We also included clade 2.2.1 A/chicken/Egypt/RIMD12-3/2008 (H5N1), referred as Ck/EG/2-3/08 (H5N1), which previously has shown to binding both 3SLN and 6SLN, after altering its polybasic CS to a monobasic CS. The monobasic CS HA of Ck/EG/2-3/08 (H5N1) also showed a consistent receptor binding profile with a previous study using the parent HA with a multibasic CS[27] (Figure 1E).

Binding for most of the H5 viruses to the human-like receptor 6SLN was undetectable (Supplementary Figure S3), except for Skua/SCO/22/22 (H5N1) which contained E185K (Figure 1F). To test the functional role of E185K in 6SLN binding, we created a mutant virus with reversion of K185E. The results confirmed that the E185K mutation increased the binding of the H5 virus to the human-like receptor 6SLN, as this phenotype was lost in the mutant (Figure 1G). To compare the avidity of the H5 virus panel for 3SLN, estimated K_d values are shown in Table S3. Compared to Ck/ENG/52/21, Skua/SCO/22/22 exhibited a 37.2-fold increase in 3SLN binding, whereas the K185E mutant of Skua/SCO/22/22 remained unchanged, suggesting that the E185K substitution enhances avidity to both 3SLN and 6SLN receptor analogues.

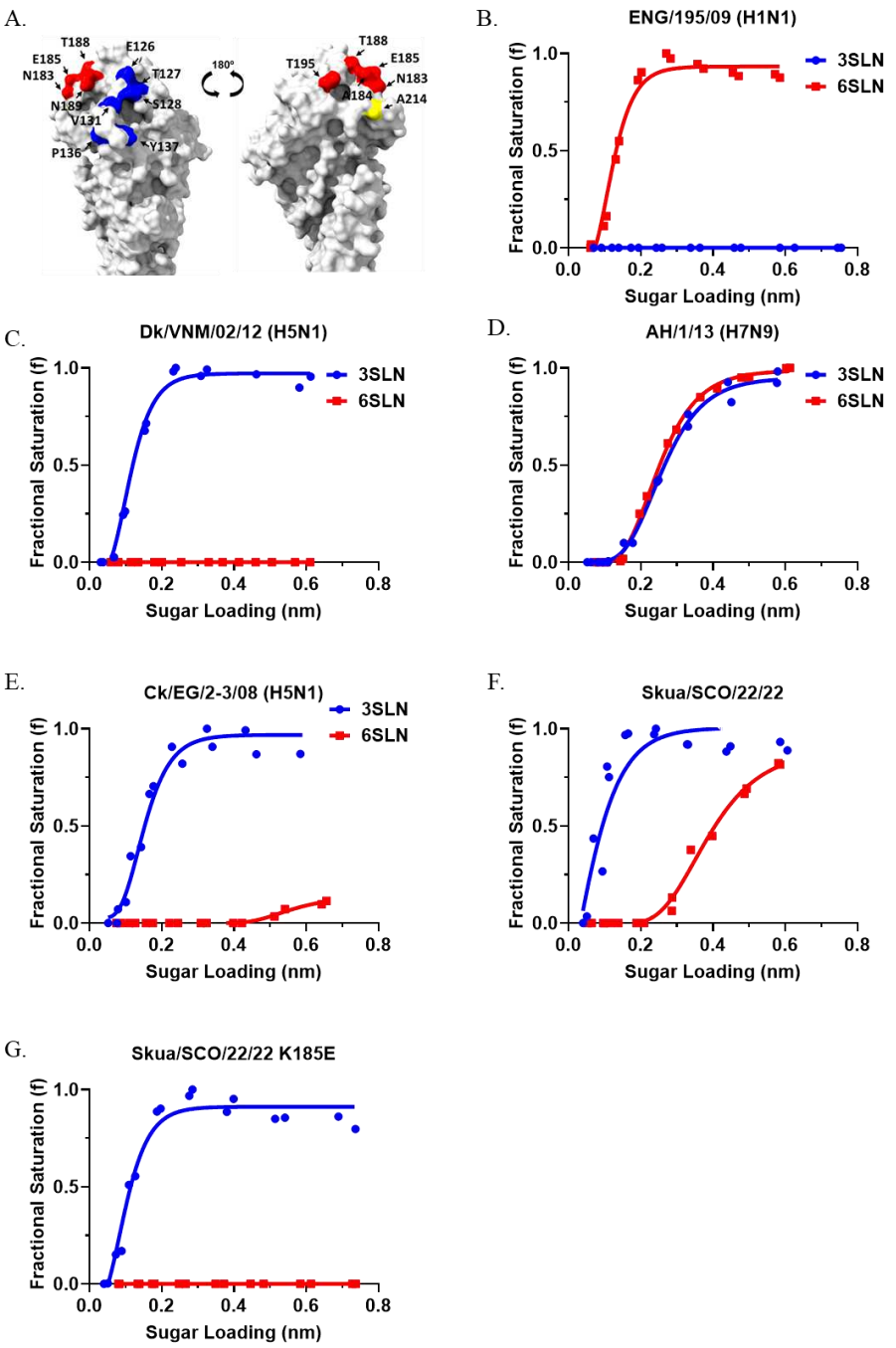


Figure 1. Receptor binding profiles of panel viruses. BLI was used to assess receptor binding of the mutant viruses with avian-like receptor analogue 3SLN (blue) and human-like receptor analogue 6SLN (red). Data points represent normalized virus binding across eight concentrations of each sugar analogue, with two replicates per concentration. Curves were fitted using an asymmetric five-parameter logistic (5PL) model. **(A)** The shortlisted amino acids are indicated by the arrows. The highlighted amino acids in 130 loop are in blue, 190 helix are in red, and 220 loop are in yellow. The viruses include: **(B)** 2009 human pandemic ENG/195/09 (H1N1), **(C)** Clade 2.3.2.1c Dk/VNM/02/12 (H5N1), **(D**) Zoonotic AH/1/13 (H7N9), **(D)** Clade 2.2.1 Ck/EG/2-3/08 (H5N1). **(F)** corresponds to Skua/SCO/22/22, and **(G)** Skua/SCO/22/22 with HA mutation K185E.

HA mutation E185K is identified as an immune escape mutant.

To evaluate evidence for the presence of diversifying positive selection across the HA RBS of clade 2.3.4.4b H5N1 viruses circulating since 2020, we estimated the ratio of rates of non-synonymous and synonymous mutations at each codon corresponding to residues of the 130 loop, 190 helix and 220 loop. To account for phylogenetic uncertainty, d_N/d_S estimates were made for a large posterior sample of time-resolved trees allowing a highest posterior density (HPD) interval to be estimated in addition to a point estimate of d_N/d_S (Fig 2A). The strongest support for positive selection was at position 185 with a mean estimate of 1.8 (95% HPD 0.9-2.7). Position 185 alone was associated with a 50% HPD interval (1.4-1.9) greater than one, whereas for the only other positions with a mean d_N/d_S estimate greater than one, 188 and 218, 50% HPD intervals spanned one, representing weaker evidence. Therefore, despite several RBS residues showing a comparable degree of amino acid variability, only position 185 has a signature suggesting diversifying positive selection. Examination of a phylogeny generated for a large sample of 2.3.4.4b viruses revealed E185K to be the most frequent non-synonymous substitution at position 185, occurring repeatedly through time and being distributed widely across the HA phylogeny (Supplementary Figure S4).

Antigenic drift in AIVs is primarily driven by mutations in HA that facilitate evasion of pre-existing anti-HA immunity derived from natural infection or vaccination. To mimic antigenic drift caused by HA mutations during vaccination in chickens and natural infection in waterfowls, we serially passaged the dominant genotype strain, Ck/ENG/52/21 (H5N1), *in-ovo* in the presence of pooled chicken post-vaccinated antiserum raised against the clade 2.3.4.4b A/crow/Aghakhan/2017 (H5N8) (Crow/Agh/17) virus, or pooled duck post-infection antiserum from Ck/ENG/52/21 (H5N1)-infected ducks to identify immune escape mutants (both viruses have HA E185) (Figure 4B). Both antisera showed comparable HI titres against Ck/ENG/52/21 (H5N1) (Supplementary Figure S5). Under continuous immune pressure with the antisera in embryonated chicken eggs, an 8-fold HI titre reduction was identified at passage 5 (p5) with duck post-infection antiserum, but there was no HI titre reduction detected at passage 10 (p10) with chicken post-vaccination antiserum (Figure 2C-2D).

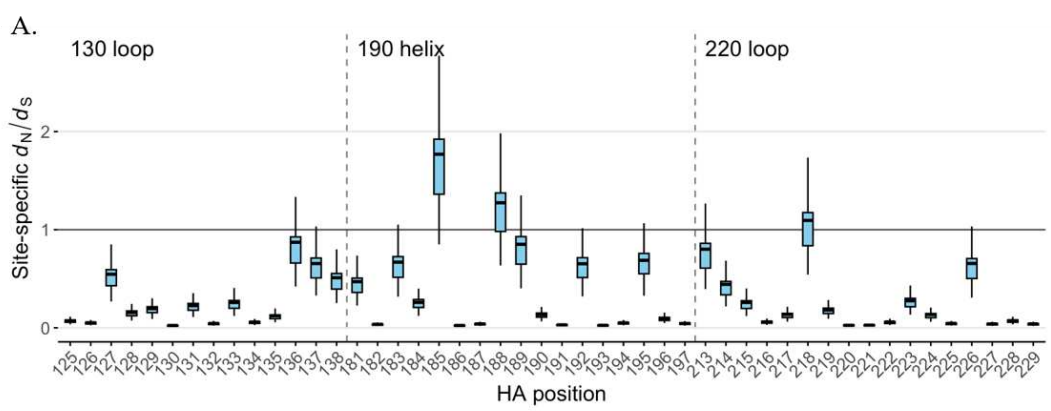
The HA gene of the p5 virus passaged in the presence of duck sera was then sequenced, and this identified the E185K mutation. A monobasic CS RG mutant virus carrying the HA E185K mutation was generated based on Ck/ENG/52/21 to confirm that the E185K mutation was the epitope change responsible for the reduction in the HI and virus neutralisation test (VNT) titres by 8-fold and 3-fold, respectively, in comparison to the Ck/ENG/52/21 (Figure 2E and 2F).

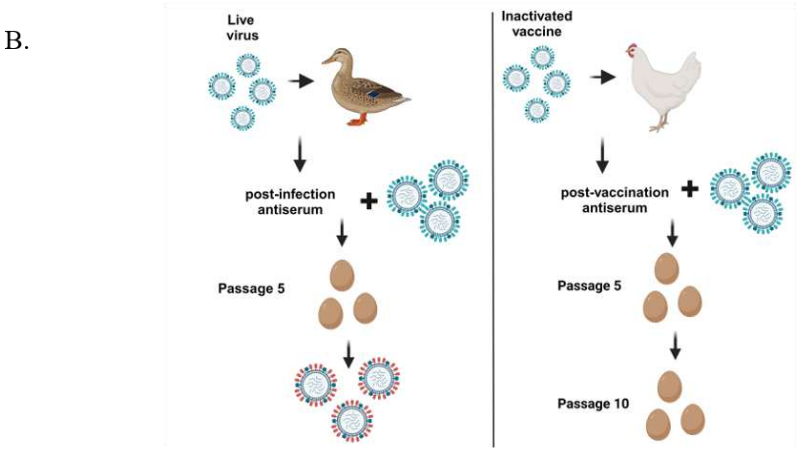
A common mechanism of immune escape in influenza is mutations that enhance HA receptor-binding avidity. Enhanced HA avidity to sialylated glycans allows this interaction to outcompete neutralisation by weaker antibodies, even when these antibodies do not bind directly to the altered epitopes[28]. We had previously found increased positive charge proximal to the receptor binding site can enhance receptor avidity[29], were therefore hypothesised E185K may act by the same mechanism. To test the effect of amino acid charge on receptor binding, we generated a panel of mutant viruses carrying E185K, E185R, E185D, E185A, or E185V, all of which have been naturally identified in the field among clade 2.3.4.4b H5Nx viruses (Supplementary Figure S6A).

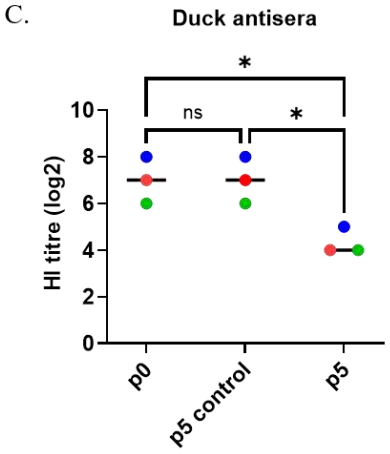
Both positively charged amino acids (E185K and E185R) showed increased avidity to both 3SLN and 6SLN compared to E185, although binding of E185R to 6SLN was weaker than that of E185K (Supplementary Figure S6B-6C). All negatively charged and neutral residues retained binding exclusively to 3SLN (Supplementary Figure S6D-F), and the estimated K_d values were also higher than E185 (Table S4). The receptor-binding profiles were further validated using elution assays with chicken and guinea pig erythrocytes, which are enriched for α-2,3 SA and α-2,6 SA receptors, respectively[30]. Compared to Ck/ENG/52/21, E185K eluted more slowly from both erythrocyte types (Supplementary Figure S6G-H), suggesting stronger binding to both α-2,3 and α-2,6 SA receptors.

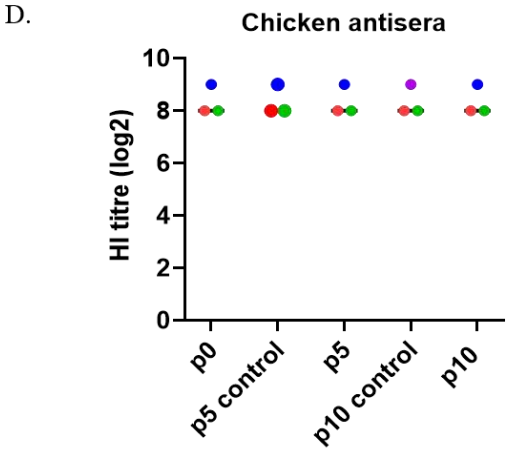
We also assessed the antigenic impact of these other E185X mutations (Supplementary Figure S7). E185A, E185R, and E185V showed significant reductions in HI titres compared to Ck/ENG/52/21, whereas E185D remained unchanged, indicating that both the identity and charge of the residue at position 185 can influence antigenicity.

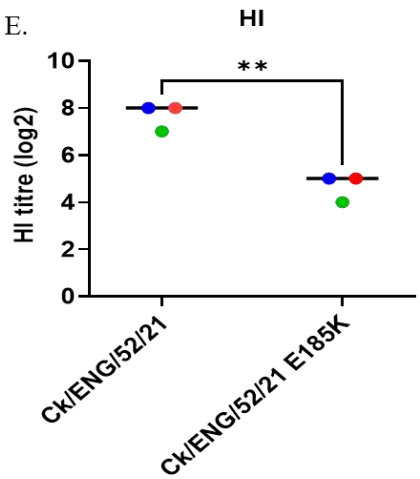
Collectively, our data identify E185K as a critical HA mutation mediating immune escape. This mutation simultaneously enhances HA receptor-binding avidity while modulating antigenicity. This highlights its potential role as a key driver of immune escape in H5Nx viruses and provides a basis for subsequent structural and functional analyses of its impact on receptor binding and antigenicity.


A.
130 loop
190 helix
220 loop
Site-specific d_N/d_S
HA position


B.
Live virus
post-infection antiserum
Passage 5
Inactivated vaccine
post-vaccination antiserum
Passage 5
Passage 10


C.
Duck antisera
HI titre (log2)
ns
*
*
p0
p5 control
p5


D.
Chicken antisera
HI titre (log2)
p0
p5 control
p5
p10 control
p10


E.
HI
HI titre (log2)
**
Ck/ENG/52/21
Ck/ENG/52/21 E185K

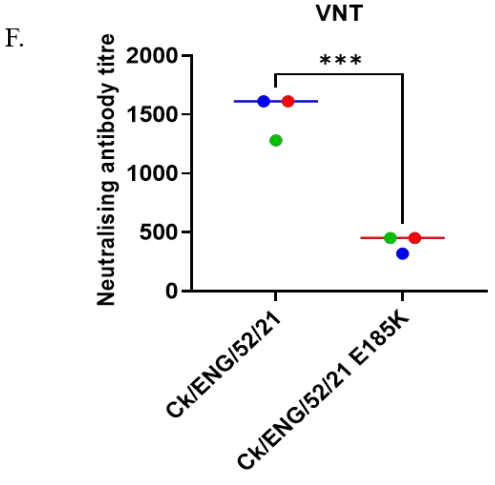

F.
VNT
Neutralising antibody titre
***
Ck/ENG/52/21
Ck/ENG/52/21 E185K

Figure 2. Selection and characterisation of HA E185K immune escape variant. (A) Positive selection analysis of HA receptor binding domains. Codon-specific ratios of relative rates of synonymous and non-synonymous substitutions (dN/dS) estimated using a renaissance counting approach integrated over a posterior sample of time-resolved phylogenies generated for sample of 824 unique H5N1 HA sequences sampled between 2020 and 2025. Box plots show the mean, boxes indicate the 50% highest posterior density (HPD) and whiskers represent the 95% HPD. (B) Schematic of immune escape variant selection. De-engineered H5N1 virus carrying a monobasic H5 HA and internal genes from the attenuated vaccine strain A/Puerto Rico/8/1934 (PR8) was passaged in chicken embryos under immune pressure with chicken post-vaccination antiserum (Crow/Agh/17 (H5N8)) or duck post-infection antiserum (Ck/ENG/52/21 (H5N1)) for up to 10 and 5 passages, respectively. (C) Haemagglutination inhibition (HI) titres of Ck/ENG/52/21 after five passages under duck post-infection antiserum. p5 virus titres are shown relative to virus passaged with uninfected duck serum and to p0 virus. (D) HI titres of Ck/ENG/52/21 virus passaged with chicken post-vaccination antiserum (Crow/Agh/17) at passages 5 (p5) and 10 (p10), compared with virus passaged with non-vaccinated chicken serum and p0 virus. (E, F) Comparison of HA E185K mutant and Ck/ENG/52/21 virus HI (D) and virus neutralisation titres (VNT, E) using duck post-infection antiserum. Data points represent biological replicates (n = 3). Statistical significance was assessed by one-way ANOVA or t test. Significance is indicated by asterisks: ns, not significant ($P > 0.05$); *, $0.05 \geqslant P > 0.01$; **, $0.01 \geqslant P > 0.001$; ***, $0.001 \geqslant P > 0.0001$; ****, $P \leqslant 0.0001$.

HA E185K has emerged upon H5N1 HPAIV circulation in cattle and also confers binding to human-like receptors in the context of the HA from cattle H5N1 viruses.

To investigate the natural occurrence of Clade 2.3.4.4b H5 viruses carrying the HA E185K mutation, we analysed all available HA sequences from this clade in GISAID collected between 1 January 2020 and 31 December 2025, a substantial proportion of cattle sequences contain E185K (Supplementary Figure S8). Phylogenetic analysis identified two distinct E185K lineages in cattle H5N1 viruses, compared with the precursor cattle H5N1 virus from Texas. In addition to the E185K mutation, one lineage contained D88G, I117F, V131M, and K234R, whereas the other contained D88G, R208K, and K212R (Figure 3A).

To determine whether cattle H5N1 viruses with HA E185K possess binding to avian- and human-like receptors, we generated RG viruses representing the two cattle lineages, as well as corresponding K185E mutants. Both cattle viruses with K185 bound to avian-like (3SLN) and human-like (6SLN) receptor analogues (Figure 3B-C), whereas the K185E mutant retained binding to 3SLN but lost detectable binding to 6SLN (Figure 3E-F).

Receptor-binding properties were further validated using a pseudovirus entry assay in HEK293T cells engineered to express the Sd^a epitope (293T-SDA), which masks α2,3-linked sialic acids, inhibiting entry of viruses that use this receptor, but not those that bind efficiently to α2,6-linked sialic acids[31,32]. Pseudovirus with H3 HA from a human virus, A/Aichi/2/1968 (H3N2), showed no reduction in entry in the 293T-SDA cells compared to 293T cells, whereas

pseudovirus with H5N1 HA from A/chicken/England/085598/2022 (Ck/ENG/98/22) or A/dairy cattle/Texas/24-008749-001/2024 (Cow/TX/01/24) showed inhibited entry. Addition of Q222L to these H5s (a known human-like receptor-adapting mutation) showed markedly increased normalised RLU in 293T-SDA cells, although entry remained higher in parental 293T cells. The Cow/TX/01/24 E185K mutant showed increased entry in 293T-SDA cells with comparable normalised RLU in both 293T and 293T-SDA cells (Figure 3F), similar to the pattern shown by pseudovirus with human H3N2 HA, suggesting that the E185K substitution reduces dependence on α2,3-linked sialic acids and facilitates entry via α2,6-linked sialic acids.

Overall, these findings indicate that the HA E185K mutation is emerging in cattle H5N1 viruses, confers enhanced binding to human-like receptors, highlighting its potential zoonotic risk.

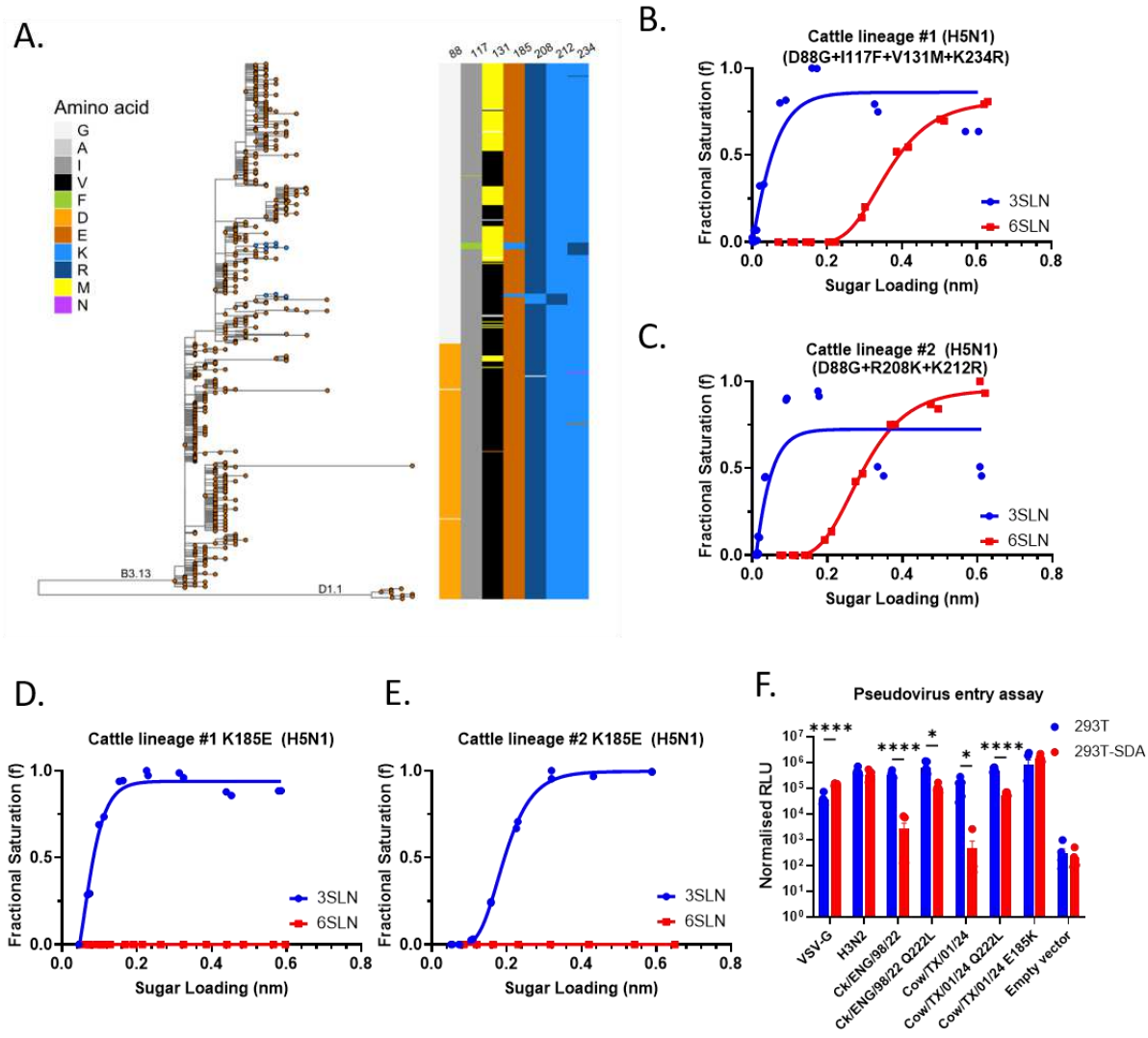


Figure 3. The emergence of HA E185K mutation in cattle. (A) Midpoint-rooted phylogeny of 484 unique H5N1 HA sequences sampled from cattle highlighting two lineages (#1 and #2) carrying

K185. Alongside, a schematic shows amino acid state at each HA site at which these two lineages differ relative to ancestral B3.13 viruses first detected in cattle. Amino acids are represented according to the key, with groups of residues with similar biophysical properties shown in shades of the same colour. (B-E) BLI was used to assess receptor binding of cattle H5N1 viruses to avian-like (3SLN, blue) and human-like (6SLN, red) receptor analogues: (D) Lineage #1 with HA D88G+I117F+V131M+K234R, (E) Lineage #2 with HA D88G+R208K+K212R, (F) Lineage #1 with HA K185E, (G) Lineage #2 with HA K185E. (H) Pseudovirus entry was quantified by luciferase assay and expressed as Relative Light Units (RLU). The assay was performed with six biological replicates. Statistical significance was assessed by one-way ANOVA and indicated by asterisks: ns, not significant ($P > 0.05$); *, $0.05 \geqslant P > 0.01$; **, $0.01 \geqslant P > 0.001$; ***, $0.001 \geqslant P > 0.0001$; ****, $P \leqslant 0.0001$.

Impact of HA mutation E185K on virus replication and stability

We next compared the growth kinetics of de-engineered monobasic CS containing H5N1 viruses, including the Ck/ENG/52/21 and its E185K mutant, both *in ovo* and *in vitro*. Replication of the E185K virus in the allantois of embryonated hens' eggs was reduced compared to that of Ck/ENG/52/21 (Figure 4A–B). Similarly, E185K showed attenuated replication compared to Ck/ENG/52/21 in all tested cell lines, including Madin-Darby canine kidney (MDCK) cells, MDCK cells stably expressing human 2,6-sialyltransferase (SIAT1; MDCK-SIAT1), chicken embryo fibroblasts (CEF), and human lung epithelial (A549) cells (Figure 4C–F). In addition, plaque assays in MDCK cells revealed that E185K formed significantly smaller plaques than Ck/ENG/52/21 (Figure 4G–H).

HA stability at low pH and high temperature is a key determinant of airborne transmission[26,33], and has previously been shown to be influenced by changes in the receptor binding domain[33,34]. We therefore assessed HA stability using syncytium formation and thermostability assays. Both Ck/ENG/52/21 and Ck/ENG/52/21 E185K viruses exhibited comparable thermostability and membrane fusion at pH 5.8 (Figure 4I–J).

We further compared the growth kinetics of de-engineered monobasic containing cattle H5N1 viruses, A/dairy cow/California/010998-001/2025 (H5N1) (Cow/CA/01/25) that naturally harbours HA K185 and its mutant virus with HA K185E and then compared their replication fitness in in human nasal epithelial cells (hNECs) from pooled donors culture at an air-liquid interface (ALI). Both viruses showed comparable replication at 16, 24 and 72 h.p.i, whereas K185E mutant showed higher replication than K185 at 48 h.p.i (Figure 4K).

Collectively, these results indicate that the E185K mutation shows no apparent evidence of increased viral replication while maintaining HA thermostability and fusion properties, suggesting a compromise between immune escape and replicative viral fitness.

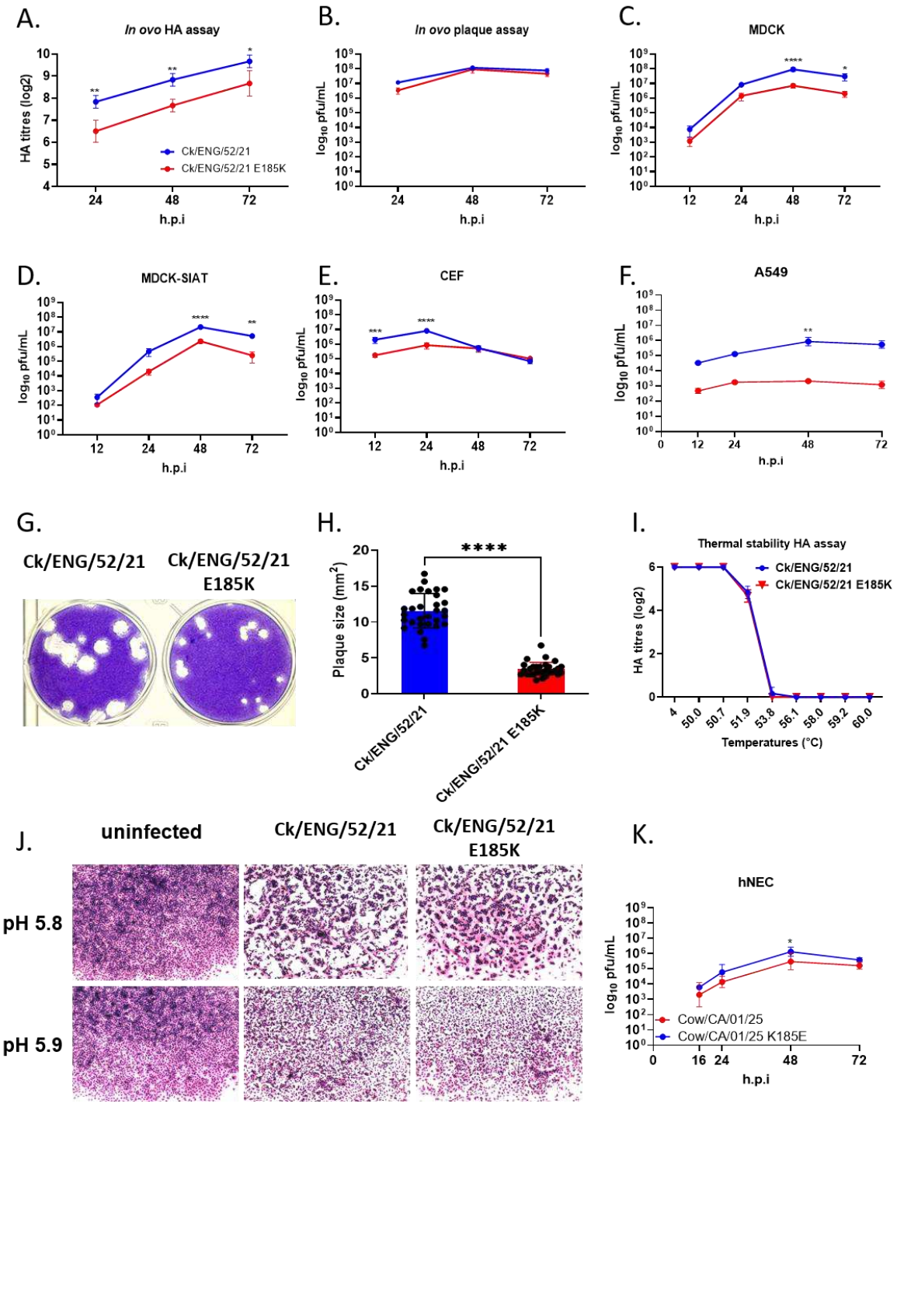

A.
In ovo HA assay
HA titres (log2)
Ck/ENG/52/21
Ck/ENG/52/21 E185K
h.p.i
B.
In ovo plaque assay
log10 pfu/mL
h.p.i
C.
MDCK
log10 pfu/mL
h.p.i
D.
MDCK-SIAT
log10 pfu/mL
h.p.i
E.
CEF
log10 pfu/mL
h.p.i
F.
A549
log10 pfu/mL
h.p.i
G.
Ck/ENG/52/21
Ck/ENG/52/21 E185K
H.
Plaque size (mm2)
****
Ck/ENG/52/21
Ck/ENG/52/21 E185K
I.
Thermal stability HA assay
HA titres (log2)
Ck/ENG/52/21
Ck/ENG/52/21 E185K
Temperatures (°C)
J.
uninfected
Ck/ENG/52/21
Ck/ENG/52/21 E185K
pH 5.8
pH 5.9
K.
hNEC
log10 pfu/mL
Cow/CA/01/25
Cow/CA/01/25 K185E
h.p.i

Figure 4. Characterisation of replication and HA stability of HA E185K H5N1 virus. Replication kinetics of de-engineered monobasic Ck/ENG/52/21 (H5N1) and its HA E185K mutant were assessed in: (A) embryonated chicken eggs by haemagglutination assay (100PFU, n = 5), (B) embryonated chicken eggs by plaque assay (100PFU, n = 5), (C) MDCK cells (0.001MOI, n = 3), (D) MDCK-SIAT1 cells overexpressing ST6 (0.001MOI, n = 3), (E) primary chicken embryo fibroblasts (CEF) (0.01MOI, n = 3), and (F) human A549 cells (0.01MOI, n = 3). (G) Plaque size comparison between Ck/ENG/52/21 and E185K viruses. (H) Representative plaque morphology of Ck/ENG/52/21 and E185K viruses. (I) Thermostability assays for Ck/ENG/52/21 and E185K viruses. (J) Syncytium formation assay to determine fusion pH of Ck/ENG/52/21 and E185K viruses. (K) Replication kinetics of de-engineered monobasic Cow/CA/01/25 and its HA K185E mutant were assessed in human nasal epithelial cells (hNECs) from pooled donors (0.01MOI, n=3). Statistical significance was assessed by two-way ANOVA or t test and indicated by asterisks: ns, not significant ($P > 0.05$); *, $0.05 \geqslant P > 0.01$; **, $0.01 \geqslant P > 0.001$; ***, $0.001 \geqslant P > 0.0001$; ****, $P \leqslant 0.0001$.

HA E185K does not increase airborne transmission in ferrets.

To further assess the airborne transmissibility of HPAIV harbouring HA K185, we used two RG HPAIVs: Cow/TX/01/24 and A/Cow/CA/01/25 (lineage #1 as described above). Cow/TX/01/24 represents the precursor B3.13 cattle H5N1 virus that naturally harbours HA E185, and Cow/CA/01/25 represents the recent emerging B3.13 cattle H5N1 virus that contains HA K185. For each virus, four ferrets were directly infected (D0) with 10^3 $TCID_{50}$ virus and co-housed with four ferrets as direct contacts (dR1), while an additional four ferrets were housed in a separate cage as indirect contacts (inR1) (Figure 5A).

Both Cow/TX/01/24 and Cow/CA/01/25 caused clinical signs which prompted euthanasia, on welfare grounds, in 100% of the directly infected ferrets. All ferrets directly infected with Cow/TX/01/24 reached humane endpoints at approximately 3 days post-infection (d.p.i.), (Mean Death time (MDT) 63h) whereas those infected with Cow/CA/01/25 had slightly delayed endpoints at around 4 d.p.i. (MDT 73.75h) One direct-contact ferret (1By) in the Cow/TX/01/24 group died, corresponding to a mortality rate of 25%, but direct contacts survived in the Cow/CA/01/25 group. No euthanasia was required among indirect-contact ferrets, for either virus (Figure 5B-C).

Oropharyngeal swabs and nasal washes were collected on alternate days to monitor virus shedding. Samples were also collected at the point of euthanasia. Apart from the directly infected ferrets and the single direct-contact ferret (1By) in the Cow/TX/01/24 group, virus shedding was not detected in any other direct-contact or indirect-contact ferrets by either oropharyngeal swab or nasal wash (Figure 5D-G).

Overall, these results indicate that both viruses were sufficiently virulent in ferrets to induce 100% mortality or euthanasia on welfare grounds, but presence of HA K185 did not confer more efficient transmission via direct and indirect airborne contact.

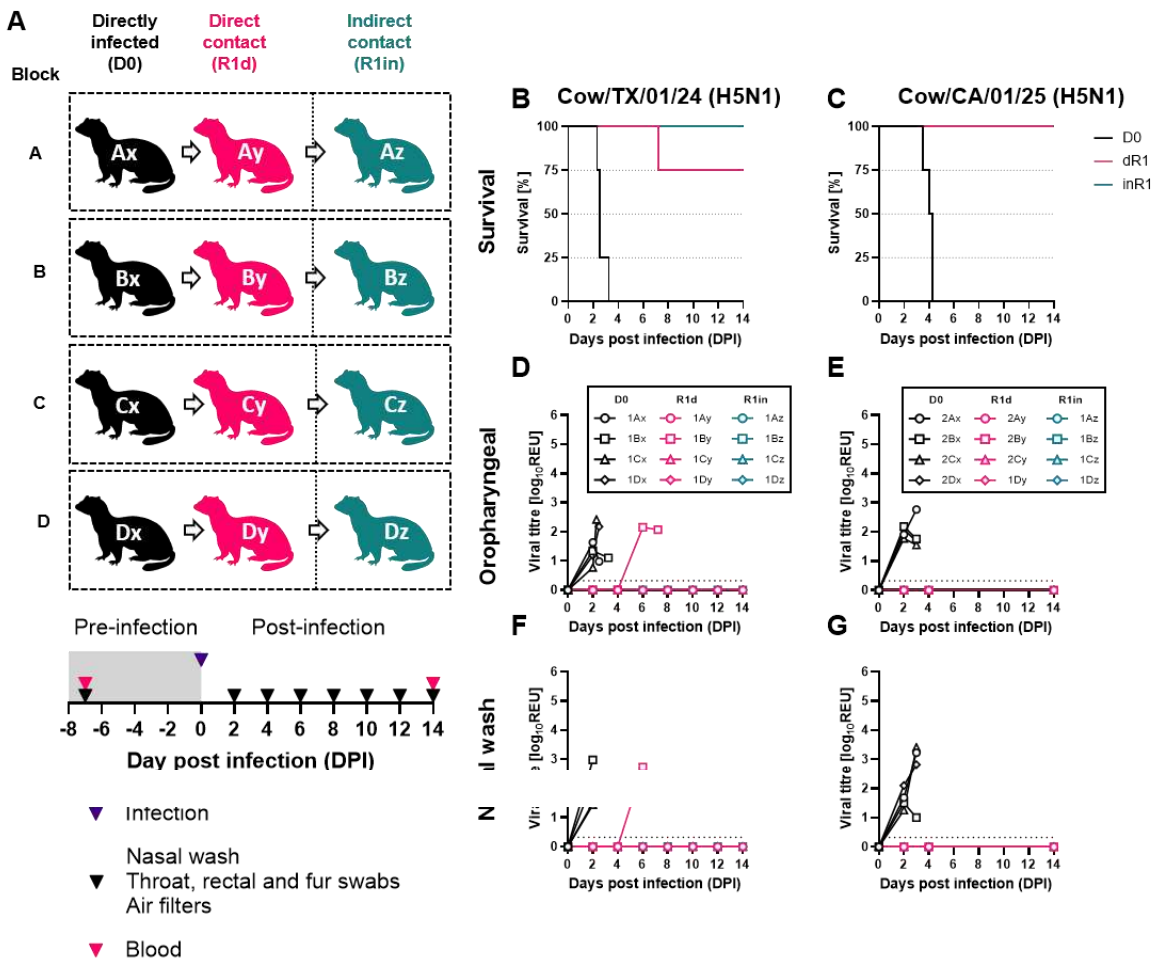


Figure 5. Viral transmission and shedding in ferrets infected with cattle-origin H5N1 viruses. (A) Schematic design of the ferret airborne transmission study. Twenty-four mixed-sex ferrets were randomly assigned to two virus groups (n = 12 per group). In each group, four ferrets were directly infected (D0) with either Cow/TX/01/24 (H5N1) or Cow/CA/01/25 (H5N1) on day 0. Four naïve ferrets were direct contacts (dR1), and an additional four naïve ferrets were housed in an adjacent cage separated by a double-mesh barrier as indirect contacts (inR1). Survival of ferrets infected with (B) Cow/TX/01/24 (H5N1) and (C) Cow/CA/01/25 (H5N1). Viral shedding detected from ferrets infected with Cow/TX/01/24 by (D) oropharyngeal swab and (F) nasal wash. Viral shedding detected from ferrets infected with Cow/CA/01/25 by (E) oropharyngeal swab and (G) nasal wash.

Discussion

Clade 2.3.4.4b H5N1 HPAI viruses continue to circulate globally, causing unprecedented outbreaks that have led to significant economic losses and substantial declines in animal populations. The influenza HA glycoprotein mediates viral entry by binding to host cell sialylated glycan receptors, as the critical step for infection. Consequently, mutations in HA can alter receptor specificity, enabling host tropism shifts and potentially facilitating cross-species transmission. Several H5 HA mutations, including H103Y, T156A, Q222L, and G224S, have been previously shown to increase virus binding to human α-2,6-SA and support airborne transmission in ferrets[17,20,33,34]. In this study, we identified a single mutation, E185K, in the HA of clade 2.3.4.4b H5N1 virus that expands receptor binding from avian-type receptors alone to increased binding of both avian- and human-type receptor analogues. Our BLI data indicate that cattle H5N1 viruses carrying K185 can bind both avian-like and human-like receptors, which is reminiscent of the dual receptor-binding 1957 pandemic H2N2 virus and the 2013 zoonotic H7N9 virus[25,35,36], highlighting its potential significance in facilitating cross-species transmission and increasing the risk of avian-to-human spillover.

We found that of all HA RBS residues, residue 185 had the strongest evidence for diversifying positive selection during the evolution of clade 2.3.4.4b H5N1 viruses since 2020. Notably, the HA E185K mutation is widespread in cattle populations, with evidence for selection and repeated emergence. HA amino acid position 185 has been identified as one of six immunodominant epitopes in clade 2.3.4.4b H5 viruses[37]. Mutations in the HA protein often arise within antigenic sites that overlap with receptor-binding domains and typically emerge as escape mechanisms under selective immune pressure. In this study, we identified E185K as immune escape variant by serially passaging an H5N1 virus in embryonated chicken eggs under pressure from clade 2.3.4.4b H5N8 post-vaccination chicken serum and H5N1 post-infection duck serum. The relevance of E185K is further supported by a recent *in-vivo* study, in which the mutation emerged in five out of six dairy cows following re-challenge with H5N1 virus[38]. Notably, the

immune escape variant was identified only using H5N1 post-infection duck serum, but not H5N8 post-vaccination chicken serum, possibly due to a mismatch of NA[39] or because convalescent serum shapes HA evolutionary landscape differently compared to antibodies induced by vaccination with whole virus[40]. Together, these findings suggest that the E185K mutation can arise under immune pressure, facilitating antibody escape and potentially contributing to viral adaptation in mammalian hosts.

The E185K mutation alters the electrostatic charge of HA, replacing a negatively charged glutamic acid with a positively charged lysine. This change enhances HA binding avidity to sialic acid receptors. Others have observed immune escape mutations include substitutions A180T and A180V (Mature HA H9 numbering) in H9N2 viruses that, while not affecting charge, increased the binding of H9N2 virus to both avian- and human-like receptor analogues by altering amino acid properties at position 180 [40,41]. Likewise, in H1N1 viruses, mutations including E156K, E158K, and E246G enabled escape from polyclonal antibody responses while significantly increasing receptor-binding avidity[28].

In this study, our ferret data showed comparable pathogenesis between two representative cattle viruses (E185 and K185) and no detectable airborne transmission from directly infected ferrets to either direct-contact or indirect-contact ferrets. This could be attributed to the pH stability of HA, particularly the threshold for HA-mediated membrane fusion, which is a key determinant of influenza virus airborne transmissibility in ferrets and a critical correlate of transmission efficiency in humans. HA from Human influenza viruses is generally more acid-stable than HA from avian viruses, with fusion activation typically occurring at pH $\leqslant$ 5.5, whereas avian viruses tend to fuse at higher pH ($\geqslant$ 5.6)[26,42]. Specific H5N1 HA mutations, including H103Y and T318I, have been reported to lower the fusion pH below 5.5, contributing to airborne transmission in ferrets[33]. In this study, we assessed the fusion pH of HA E185K mutation and found that the virus fused at pH 5.8, indicating that E185K does not increase HA acid stability. Our recent study has shown emerging HA mutation D88G in cattle H5N1 lowered the fusion pH to 5.6, within the typical pH range for avian influenza viruses[43]. The RG HPAIV A/Cow/CA/01/25 used in this study, which naturally harbours G88 and K185 in combination, is unlikely to enhance airborne transmission in ferrets. Given the strong association between HA acid stability and transmission, continued surveillance and functional assessment of pH-stabilising mutations in contemporary clade 2.3.4.4b H5 HA glycoproteins remains a priority, especially when combined with mutations that confer binding to human-type sialic acid receptors.

In conclusion, we identified HA E185K as an immune escape mutation in clade 2.3.4.4b H5N1 viruses that confers increased binding to avian- and human-type receptors and has

become prevalent in cattle-origin H5N1 viruses. While E185K independently does not significantly enhance pathogenesis in the ferret model, or enhance airborne transmission, its emergence in combination with other adaptive mutations may pose increased zoonotic risk. Potential H5N1 vaccination and sustained B3.13 infection in US dairy cattle, with most animals surviving infection and developing population-level immunity, may influence future viral evolution. These findings emphasise the importance of continued surveillance and functional characterisation of emerging H5N1 variants to better assess their potential for cross-species transmission and public health impact.

Methods

Ethics and biosafety

All the procedures involving embryonated eggs, chickens and ferrets were carried out in strict accordance with the guidance and regulations of United Kingdom Home Office regulations under project licences PP671846, PP7633638 and PP97878849. As part of this process, the work has undergone scrutiny and approval by the Animal Welfare Ethical Review bodies at the Pirbright Institute (TPI) and the Animal and Plant Health Agency (APHA). The study designs incorporated the 3Rs principles and the ARRIVE (Animal Research: Reporting of *in vivo* experiment) guidelines for quality, reproducibility and translatability of animal studies.

All the influenza virus-related work was carried out at containment level 2 (CL2) conditions for reverse genetics-generated de-engineered virus containing monobasic CS H5 HA and homologous NA, and internal genes from attenuated vaccine strain A/Puerto Rico/8/1934 (PR8). Work related with full reverse genetics-generated virus containing multibasic CS H5 HA was performed at CL3 conditions in licensed specified animal pathogens order (SAPO) 4 and Advisory Committee on Dangerous Pathogens (ACDP) 3 facilities at TPI and APHA following United Kingdom regulations.

Cells and viruses

MDCK, MDCK-SIAT1, human embryonic kidney 293T (HEK-293T), African green monkey kidney epithelial (Vero), A549 and CEF cells were acquired from Cell Services Unit (CSU) of TPI. MDCK, MDCK-SIAT1, HEK-293T, Vero and A549 Cells were maintained with Dulbecco's Modified Eagle's medium (DMEM) supplemented with 10% foetal calf serum (FCS) (Gibco). CEF cells were cultured with medium 199 supplemented with 5% FCS and 5% Tryptose Phosphate Broth (TPB). Human airway cultures (HNECs) in air-liquid interface (ALI) were derived from a pool of 14 healthy human donors (Epithelix MucilAir™-Pool nasal, batch: MP0012). HNECs were cultured in 24-well

plates, following supplier instructions to remove cells from agarose. Cells were washed with PBS and given fresh media every 48hrs using MucilAir™ medium (Epithelix)[44]. All cell cultures were maintained at 37 °C with 5% CO_2.

The polybasic CS of H5 HA was replaced with the monobasic PLGTR/GLF CS for the study to be conducted at CL2. The HA and NA sequences of clade 2.3.4.4b H5Nx viruses used in this study were acquired from NCBI and GISAID[45]. The source of virus sequence (GISAID/NCBI), isolate ID, submitting laboratory, originating laboratory, and author details are listed in Table S1, while the HA amino acid differences among the panel viruses are provided in Table S2, with changes highlighted in red. The HA of A/duck/Vietnam/OIE-2202/2012 (H5N1) and A/chicken/Egypt/RIMD12-3/2008 (H5N1) were acquired from NCBI with accession number AB769252 and AB601123, respectively. HA plasmids with polybasic CS were generated in SAPO4/ACDP3 CL3 containment at TPI by changing the CS from monobasic to polybasic. All accession numbers and details for the HPAIV segments used in this study are listed in table S5. The sequences were synthesised by GenScript and further cloned into the bi-directional pHW2000 vector. The desired HA mutations were generated using single-site mutagenesis QuikChange II kit (Agilent) following manufacturer's instructions. The viruses were rescued by the eight-plasmid approach as previously described[46]. RG A/England/195/2009 (H1N1) and RG A/Anhui/1/2013 (H7N9) were generated as previously described[47,48].

For ferret work, RG generated viruses (A/dairy cattle/Texas/24-008749-002/2024, A/dairy cow/USA/010998-001/2025) were propagated in embryonated chicken eggs. Virus titre was determined by TCID50 on MDCK cells, and sequences confirmed using Oxford Nanopore Technologies (ONT) before infection.

Virus purification and quantification

ENG/195/09 (H1N1) was propagated in MDCK cells, and all other viruses were propagated in 9- or 10-day old embryonated chicken eggs. The propagated viruses were then pelleted at 27,000 rpm for 2 hr at 4°C. Pelleted viruses were then purified through a 30%-60% sucrose gradient for 2 hr at 4°C. Purified viruses were resuspended in PBS and quantified by enzyme-linked immunosorbent assay (ELISA) as previously described by comparing to viral nucleoprotein detection to a known standard[49].

Bio-layer interferometry (BLI)

The receptor binding was assessed with Bio-layer interferometry (BLI) as previously described[50]. Briefly, 100 pmol of purified viruses quantified by ELISA were diluted with HBS-EP

buffer (TEKnova) supplemented 10 μM oseltamivir carboxylate (Roche) and 10 μM zanamivir (GSK). The receptor binding was tested with Octet® R8 system (Sartorius) using streptavidin biosensors (Sartorius). Avian-like sugar analogues α-2,3-sialyllactosamine (3SLN) and human-like sugar analogue α2,6-sialyllactosamine (6SLN) were purchased from GlycoNZ, and used for the detection. Virus binding affinity was normalised to fractional saturation and the concentrations of sugar loadings[50].

Selection of immune-escape variants

The selection of immune-escape variants was described previously with minor modifications[48]. In brief, 100μL containing 32 haemagglutinating units (HAU) of de-engineered Ck/ENG/52/21 (H5N1) was incubated with 100 μL of pooled chicken post-vaccinated antisera or pooled duck post-infection antisera at serial dilutions at 37°C for 1 hr in duplicates. Non-vaccinated chicken and non-infected duck sera were used as negative controls.

The virus-antiserum mixtures were then inoculated into 9- to 10-day-old embryonated chicken eggs for 48 hr. The eggs were subsequently chilled overnight at 4°C, and allantoic fluid was harvested for haemagglutination assays. Samples that showed haemagglutination titres at the lowest antiserum dilution selected for further passage. Passaging with chicken post-vaccination antisera was repeated 10 passages, and for 5 passages with duck post-infection antisera.

Viral RNA of the passaged virus was extracted using the QIAamp Viral RNA Minikit (Qiagen). Viral RNA was converted to cDNA with the Verso cDNA synthesis kit (Thermo Scientific). The HA segment was amplified using pfu Ultra high-fidelity DNA polymerase (Agilent) and cloned into the pCR-Blunt vector following the instructions of the Zero Blunt PCR Cloning Kit (Thermo Fisher Scientific). The plasmids were transformed into DH5α competent cells, colonies were then picked, and inserts were confirmed by Sanger sequencing.

Antisera preparation

Duck polyclonal post-infection (convalescent) antisera were generated from previous *in vivo* experiments using a H5N1 clade 2.3.4.4b HPAIV[51]. Chicken polyclonal antisera against Crow/Agh/17 (H5N8) were prepared as previously described[52]. In brief, egg-propagated virus was inactivated with 0.1% (v/v) β-propiolactone (BPL) and then concentrated by ultracentrifuge at 27,000 rpm for 2 hr at 4°C. Three-day-old specific pathogen free (SPF) chickens were intramuscularly vaccinated with 1024 HAU of inactivated concentrated virus mixed with oil immersion adjuvant (Montanide; Seppic) at a adjuvant : virus 7:3 ratio. A boost dosage was given

after 10 days. The inoculated chickens were wing bled at 18-, 25- and 38-days post-inoculation for HI validation. The birds were culled at 42 days post-inoculation and serum samples were collected and stored in aliquots at -20°C.

Haemagglutination (HA) Assay

HA titres were determined using standard haemagglutination assays[53]. Briefly, 50 µL of two-fold serially diluted virus in phosphate-buffered saline (PBS) was added to a 96-well V-bottom plate. An equal volume (50 µL) of 1% chicken red blood cells (RBCs) was added to each well, and the plates were gently mixed. After 30 minutes of incubation at room temperature, HA titres were recorded as the highest virus dilution that produced complete agglutination of RBCs. All assays were performed in duplicate to ensure reproducibility.

Haemagglutination Inhibition (HI) Assay

HI assays were performed to assess the ability of antisera to inhibit virus-induced agglutination[53]. Two-fold serial dilutions of serum (25 µL per well) were mixed with an equal volume (25 µL) of virus containing 4 HAU and incubated for 30 minutes at room temperature. Subsequently, 50 µL of 1% RBC suspension was added, and the mixture was incubated for an additional 30 minutes. The HI titre was recorded as the highest serum dilution that completely inhibited haemagglutination. All assays were performed in duplicate.

Virus Neutralisation Test (VNT)

Serial two-fold dilutions of antisera were prepared in DMEM. Each serum dilution (50 µL) was mixed with an equal volume of virus containing 100 $TCID_{50}$ and incubated at 37 °C for 1 hour to allow virus–antibody interaction. Confluent monolayers of MDCK cells in 96-well plates were then infected with 100 µL of the virus–serum mixture and incubated at 37 °C for 1 hour. After adsorption, the inoculum was removed, cells were washed three times with PBS, and 100 µL fresh DMEM containing N-tosyl-L-phenylalanine chloromethyl ketone (TPCK)-treated trypsin was added. Plates were incubated for 3 days at 37 °C. After incubation, cells were fixed and stained with 0.1% crystal violet to visualise cytopathic effect (CPE). The VNT titre was defined as the highest serum dilution that completely prevented virus-induced CPE in at least 50% of the wells. All assays were performed in duplicate, and mean titres were calculated.

Virus Replication kinetics and plaque assay titration

MDCK and MDCK-SIAT1 cells were infected with H5N1 viruses at a multiplicity of infection (MOI) of 0.001, whereas chicken embryo fibroblast (CEF) and A549 cells were infected at an MOI of 0.01. Infected cells were incubated at 37 °C for 1 h, washed three times with PBS, and cultured in DMEM containing TPCK-treated trypsin (2 µg/mL for MDCK and MDCK-SIAT1 cells; 0.2 µg/mL for CEF and A549 cells). Supernatants were collected at 12, 24, 48, and 72 hr post-infection (hpi).

Infection of primary human nasal epithelial cells (hNECs) cultured at an air–liquid interface was performed as previously described[54]. Briefly, cells were infected with virus at an MOI of 0.01 in Dulbecco's phosphate-buffered saline supplemented with calcium and magnesium (DPBS++) at 37°C for 1 hr. Virus-containing supernatants were collected by adding 200 µL of DPBS++ to the apical surface, incubating for 10 min at 37°C, and subsequently removing the wash for titration.

Collected supernatants were titrated by plaque assay on MDCK cells as described previously[55]. Briefly, confluent MDCK monolayers in 12-well plates were washed three times with PBS and infected with ten-fold serial dilutions of supernatants prepared in DMEM for 1 hr at 37°C. Following infection, the inoculum was removed and cells were overlaid with medium containing 0.6% agarose (Thermo Fisher), 1× MEM, 100 U/mL penicillin, 100 µg/mL streptomycin, 2 mM L-glutamine, 0.3% bovine serum albumin (BSA), 15 mM HEPES, 0.22% sodium bicarbonate, and 0.01% DEAE-dextran (Sigma-Aldrich). After 72 hr incubation at 37°C, cells were fixed with 4% paraformaldehyde and plaques were visualised by staining with 1% crystal violet (Sigma-Aldrich) in 20% methanol. Plaques were counted manually, and virus titres were calculated as plaque-forming units per millilitre (PFU/mL) based on the dilution factor and inoculum volume.

In ovo replication kinetics

Nine-day-old specific-pathogen-free (SPF) embryonated chicken eggs were inoculated via the allantoic cavity with 100 PFU of virus in a volume of 100 µL. Inoculated embryos were incubated at 37°C. At 24, 48, and 72 hr post-infection (hpi), embryos (n = 5 per group per time point) were euthanised by chilling at 4°C overnight. Allantoic fluid was subsequently harvested and used for downstream haemagglutination and plaque assays.

Thermostability assay

Viruses were diluted with sterile allantoic fluid to 32 HAU/50µL. The diluted viruses were next incubated in thermal cycler (Bio-Rad) at 50°C, 50.7°C, 51.9°C, 53.8°C, 56.1°C, 58.0°C,

59.2°C, and 60°C and 4°C as control for 30 min. The HA titres were then determined by haemagglutination assay as described above.

Syncytium formation assays

The syncytium formation assays were performed as previously described[55]. Vero cells were infected with 1.0 multiplicity of infection (MOI) of each virus for 1 hr at 37°C. The infected cells were then incubated at 37°C for 15 hr after washing with PBS for three times. The cells were then treated with 3.0 µg/mL TPCK trypsin in DMEM for 15 min and followed by incubation with PBS ranging from pH 5.2 to 6.0 at 0.1 pH increment for 5 min. The cells were then washed with DMEM and maintained with DMEM media supplemented with 10% FCS for 3 hr. The cells were then fixed with acetone: methanol (1:1 ratio) and stained with Giemsa overnight at room temperature (Sigma-Aldrich). Stained cell images were taken by EVOS XL imaging system at 400 µm (Life Technologies). The lowest pH that induced visible syncytium formation is recorded as the pH of fusion with multinucleated cells and indistinct cell membranes.

Production of pseudoviruses

The VSV-G expression plasmid, and lentiviral packaging genes and luciferase genome were used as previously described[56]. The following human codon optimised HA, NA, protease and sialyl-transferase expression plasmids were synthesised by Genscript in pcDNA3.1: H5 HA - A/dairy cattle/Texas/24-008749-001/2024 (H5N1; WPD27583.1), H5 HA - A/chicken/England/085598/2022 (H5N1; EPI2089022) (referred to as Ck/ENG/98/22), H3 HA – A/Aichi/2/1968 (H3N2; BAF37221.1), and human TMPRSS11D/HAT (EAX05559.1). Pseudoviruses expressing HA were produced in HEK293Ts seeded in six well plates. Cells were transfected with lipofectamine 3000, 0.4 µg HA or VSV-G, 0.4 µg of the HIV packaging plasmid (pGAG-POL), 0.6 µg of a luciferase reporter construct (pCSFLW), and 0.2 µg of TMPRSS11D (H3 only). After 24 hr, one unit of neuraminidase from *Clostridium perfringens* (Sigma-Aldrich, N2876) was added to fresh media to induce virus budding. After 48 hr, pseudovirus containing supernatant was collected and filtered through a sterile 0.45 µm Millex®-HA filter unit.

Pseudovirus entry assay

All pseudoviruses were titrated before use in entry assays as previously described[57]. Pseudoviruses were added in duplicate to a white Nunc™ MicroWell™ 96-well, flat-bottom microplate with 50 µL pseudotyped influenza virus per well (diluted in media to reach a standard titre of 1×10^6 RLU after 48 hr, based on the virus titrations). Pseudoviruses were incubated at 37 °C with 50 µL of $1x10^5$ cells: either wild-type HEK239T cells or HEK293T-SDA cells

(Supplementary S9). 48 hr post-transduction cells were lysed with Bright-Glo™ Luciferase Assay System (Promega). The RLU of the cell lysate was determined using the FLUOstar OMEGA microplate reader (BMG Labtech).

Ferret study

Twenty-four mixed-sex ferrets (*Mustela putorius furo*) aged approximately 2 months weighing from 500 g to 750 g were selected and implanted with microchips to monitor ferret ID and body temperature. The ferrets were confirmed to be seronegative for influenza A virus using the ID Screen Influenza A Nucleoprotein Indirect ELISA (ID Vet) and were further shown to be uninfected by M-gene RT-qPCR performed on nasal wash samples[58].

The ferrets were randomly distributed into two virus groups (n = 12 per group), with litter mates separated where information was available. Within each virus group, 4 ferrets were directly infected (D0), 4 served as direct contacts (dR1), and 4 served as indirect contacts (inR1). Ferrets were assigned unique identifiers based on virus group and transmission category.

For the Cow/TX/01/24 group, the directly infected ferrets were designated 1Ax, 1Bx, 1Cx, and 1Dx. The corresponding direct contact ferrets were designated 1Ay, 1By, 1Cy, and 1Dy, while the indirect contact ferrets were designated 1Az, 1Bz, 1Cz, and 1Dz. Similarly, in the Cow/CA/01/25 group, the directly infected ferrets were designated 3Ax, 3Bx, 3Cx, and 3Dx; the direct contacts were designated 3Ay, 3By, 3Cy, and 3Dy; and the indirect contacts were designated 3Az, 3Bz, 3Cz, and 3Dz.

The directly infected ferrets (n=4) were intra nasally challenged with 10^3 $TCID_{50}$ of either Cow/TX/01/24 or Cow/CA/01/25 on day 0, and returned to cages with cohoused direct contact, and separated indirect contacts. Oropharyngeal swab and nasal wash were collected in PBS or L-15 (Gibco) respectively on alternate days for 14 days, and the ferrets were culled and heart bled on day 14. Total RNA was extracted from the respiratory samples and tested by the H5-HPAIV-specific RT-qPCR to assess viral shedding[59].

Haemagglutinin structure prediction

The structure of H5 HA was acquired from Protein Data Bank (https://www.rcsb.org/). The accession of the HA is 4JUL. HA structure modelling and prediction were visualised in UCSF ChimeraX as previously described[60].

Phylogenetic analysis

All influenza A H5 HA sequences with submission dates between and 1st January 2020 and 27th June 2025 were downloaded from GISAID[45].Nucleotide sequences were aligned using MAFFT v7.511[61]. Sequences of clade 2.3.4.4b with nucleotide coverage over 0.95 were retained. Those resulting from environmental sampling or inferred to be laboratory-derived reassortant viruses were excluded. Furthermore, sequences from avian hosts with imprecise host information such as 'avian' or 'wild bird' were also excluded.

To investigate site-specific signatures of selection across the receptor-binding regions of HA, a stratified sample of H5N1 HA sequences with full information on sampling date and nucleotide sequence at each receptor-binding residue was generated. This sample consisted of one randomly selected sequence per country per month from which 824 unique HA sequences were analysed. Codon-specific ratios of relative rates of synonymous and non-synonymous substitutions (d_N/d_S) were estimated using a renaissance counting approach[62]. This approach integrates over a posterior distribution of time-scaled phylogenies. Estimates of d_N/d_S greater or less than one provides evidence for either diversifying, positive or purifying selection, respectively. Renaissance counting was performed with a general time reversible (GTR) model of nucleotide substitution partitioned to allow base frequencies and substitution rate parameters to vary at each codon position, a strict molecular clock, and a Bayesian SkyGrid tree prior with 12 parameters and a time at last transition of 6 years, implemented in BEAST v1.10.4[63]. Two chains were checked for convergence and that all effective samples sizes on parameters exceeded 200. Highest posterior density intervals were estimated using the R package HDInterval v0.2.4[64].

To investigate broader trends at position 185 across H5Nx clade 2.3.4.4b evolution, a stratified sample of the larger set of processed clade 2.3.4.4b HA sequences described above was generated. This consisted of one sequence randomly selected for each combination of country sampled, month and amino acid state at 185. From the resulting set of 1,144 sequences, a time-scaled phylogeny was estimated using Delphy v1.0.3 (https://github.com/fathominfo/delphy-web) with sequence evolution modelled using a GTR model with site heterogeneity drawn from a continuous gamma distribution. Delphy was run for over 5,000 million steps sampling every 10 million steps and the minimum effective sample size exceeded 400. The maximum clade credibility tree was identified using TreeAnnotator v1.10.4[63], and visualised in R[65] using the ggtree package[66] .

To examine amino acid variation at HA position 185 among sequences derived from dairy cattle, 3,644 sequences from either 2024 or 2025, with host determined as being labelled as either 'cattle' or 'dairy cow' and nucleotide coverage for the codon corresponding to position 185

were identified. Of these, 484 unique nucleotide sequences (ignoring gap characters) were identified and from these, phylogeny was estimated with a GTR model using FastTree v2.2.0[67,68].

Statistical analysis

Data analysis and visualisation were conducted using GraphPad Prism 10.0 (GraphPad Software, USA). Unpaired t-test, ordinary one-way ANOVA Dunnett's multiple comparisons test, and two-way ANOVA multiple comparisons were used for statistical significance determination. One asterisk indicates $0.01 \leq p < 0.05$, and $0.001 \leq p < 0.01$, $0.0001 \leq p < 0.001$ and $p < 0.0001$ having two, three or four asterisks, respectively. $p > 0.05$ was considered not significant.

Data Availability Statement

All raw experimental data supporting the findings of this study are available from the corresponding author upon reasonable request. Viral sequence data analysed in this study were obtained from GISAID and NCBI. Plasmids, recombinant viruses, and other materials are available upon reasonable request, subject to institutional intellectual property policies and biosafety regulations.

Acknowledgments & Funding Acquisition

We gratefully acknowledge all data contributors, i.e., the Authors and their Originating laboratories responsible for obtaining the specimens, and their Submitting laboratories for generating the genetic sequence and metadata and sharing via the GISAID Initiative, on which this research is based. All submitters of the data may be contacted directly via the GISAID website (https://www.gisaid.org). All the virus metadata used in this study, including isolate name, ID, segment ID, submitting lab, originating lab and authors are listed in Table S1. We would like to thank Professor Nicholas S. Heaton of Duke University School of Medicine for sharing B4GALNT2 containing plasmid. We thank Dr. Steve Martin for sharing Octet analysis software for receptor binding analysis. We thank Benjamin Mollett, Kajal Ralh, Caroline Warren, Amy Miller, Katie Brown, and Sarah Tamasauskas for help with the ferret studies. The schematic graphs were generated from BioRender.

This work was supported by UK Research and Innovation (UKRI) Biotechnology and Biological Sciences Research Council (BBSRC) /DEFRA "FluMAP" (BB/X006123/1) 'FluTrailMap' [BB/Y007298/1 and BB/Y007352/1] and FluTrailMap-One Health [MR/Y03368X/1] consortia. MI, IHB, TPP, J Yang, KRV, TKK, MQ, SR, TC and JRS are also supported by the BBSRC funded Pirbright Institute's Strategic Programme Grants (ISPGs) [BBS/E/PI/230001A; BBS/E/PI/230002A;

BBS/E/PI/230002B; BBS/E/PI/230001C; BBS/E/PI/23NB0004; BBS/E/PI/23NB0003] and High Containment and Low Containment Services and Science Platforms grants [BBS/E/PI/23NB0004, BBS/E/PI/23NB0003]. WTH, PD and SJL are also supported by the BBSRC-funded Roslin Institute's ISPG grants [BBS/E/D/20002173; BBS/E/D/20002174]. ACB, JJ, MS and PD further acknowledge support from Defra in the form of the ICRAD project "FluSwitch" (SE2223), while PD acknowledges support by UKRI Medical Research Council (MRC) grant (MR/Y015045/1). J Yu and YL acknowledge funding from The UK Medical Research Council grant [MR/R010757/1] The funders had no role in study design, data collection, data interpretation, or the decision to submit the work for publication.

Competing Interests Statement

The authors declare no competing interests.

Author Contributions

Funding acquisition: CS, YL, MJS, ACB, TTP, IHB, PD, SJL, WSB, JJ and MI;
Conceptualisation: J Yang, WTH, ACB, TTP, IHB, SJL, WSB, JJ and MI;
Methodology: J Yang, EB, SR, WTH, SJ, KRV, HK, KS, J Yu, TKK, MQ, SASR, TC, JH, CDG, GW, KR, JRS, DEDPH, TM, MW;
Data curation: J Yang, EB, WTH, KRV, HK, J Yu, JJ;
Visualisation: J Yang, EB, WTH, HK, JJ
Formal analysis: J Yang, EB, WTH, HK, JJ
Writing-original draft: J Yang, EB, WTH, HK
Writing-editing: All authors

Reference

1 Claas, E. C. *et al.* Human influenza A H5N1 virus related to a highly pathogenic avian influenza virus. *Lancet* **351**, 472–477 (1998). https://doi.org/10.1016/S0140-6736(97)11212-0

2 Subbarao, K. *et al.* Characterization of an avian influenza A (H5N1) virus isolated from a child with a fatal respiratory illness. *Science* **279**, 393–396 (1998). https://doi.org/10.1126/science.279.5349.393

3 Xie, R. *et al.* The episodic resurgence of highly pathogenic avian influenza H5 virus. *Nature* **622**, 810–817 (2023). https://doi.org/10.1038/s41586-023-06631-2

4 Zeng, J. *et al.* Spatiotemporal genotype replacement of H5N8 avian influenza viruses contributed to H5N1 emergence in 2021/2022 panzootic. *J Virol* **98**, e0140123 (2024). https://doi.org/10.1128/jvi.01401-23

5 Harvey, W. T. *et al.* Genetic reassortment and diversification of host specificity have driven evolutionary trajectories of lineages of panzootic H5N1 influenza. *bioRxiv*, 2025.2008.2020.670882 (2025). https://doi.org/https://doi.org/10.1101/2025.08.20.670882

6 Briand, F. X. *et al.* Highly Pathogenic Clade 2.3.4.4b H5N1 Influenza Virus in Seabirds in France, 2022-2023. *Transbound Emerg Dis* **2025**, 8895883 (2025). https://doi.org/10.1155/tbed/8895883

7 Greco, F. *et al.* Asymptomatic infection and antibody prevalence to co-occurring avian influenza viruses vary substantially between sympatric seabird species following H5N1 outbreaks. *Sci Rep* **15**, 1435 (2025). https://doi.org/10.1038/s41598-025-85152-6
8 Rijks, J. M. *et al.* Highly Pathogenic Avian Influenza A(H5N1) Virus in Wild Red Foxes, the Netherlands, 2021. *Emerg Infect Dis* **27**, 2960–2962 (2021). https://doi.org/10.3201/eid2711.211281
9 Aguero, M. *et al.* Highly pathogenic avian influenza A(H5N1) virus infection in farmed minks, Spain, October 2022. *Euro Surveill* **28** (2023). https://doi.org/10.2807/1560-7917.ES.2023.28.3.2300001
10 Rabalski, L. *et al.* Emergence and potential transmission route of avian influenza A (H5N1) virus in domestic cats in Poland, June 2023. *Euro Surveill* **28** (2023). https://doi.org/10.2807/1560-7917.ES.2023.28.31.2300390
11 Uhart, M. M. *et al.* Epidemiological data of an influenza A/H5N1 outbreak in elephant seals in Argentina indicates mammal-to-mammal transmission. *Nat Commun* **15**, 9516 (2024). https://doi.org/10.1038/s41467-024-53766-5
12 Burrough, E. R. *et al.* Highly Pathogenic Avian Influenza A(H5N1) Clade 2.3.4.4b Virus Infection in Domestic Dairy Cattle and Cats, United States, 2024. *Emerg Infect Dis* **30**, 1335–1343 (2024). https://doi.org/10.3201/eid3007.240508
13 Baker, A. L. *et al.* Dairy cows inoculated with highly pathogenic avian influenza virus H5N1. *Nature* **637**, 913–920 (2025). https://doi.org/10.1038/s41586-024-08166-6
14 Gamblin, S. J. & Skehel, J. J. Influenza hemagglutinin and neuraminidase membrane glycoproteins. *J Biol Chem* **285**, 28403–28409 (2010). https://doi.org/10.1074/jbc.R110.129809
15 Costa, T. *et al.* Distribution patterns of influenza virus receptors and viral attachment patterns in the respiratory and intestinal tracts of seven avian species. *Vet Res* **43**, 28 (2012). https://doi.org/10.1186/1297-9716-43-28
16 Walther, T. *et al.* Glycomic analysis of human respiratory tract tissues and correlation with influenza virus infection. *PLoS Pathog* **9**, e1003223 (2013). https://doi.org/10.1371/journal.ppat.1003223
17 Chutinimitkul, S. *et al.* In vitro assessment of attachment pattern and replication efficiency of H5N1 influenza A viruses with altered receptor specificity. *J Virol* **84**, 6825–6833 (2010). https://doi.org/10.1128/JVI.02737-09
18 Gao, Y. *et al.* Identification of amino acids in HA and PB2 critical for the transmission of H5N1 avian influenza viruses in a mammalian host. *PLoS Pathog* **5**, e1000709 (2009). https://doi.org/10.1371/journal.ppat.1000709
19 Wang, W. *et al.* Glycosylation at 158N of the hemagglutinin protein and receptor binding specificity synergistically affect the antigenicity and immunogenicity of a live attenuated H5N1 A/Vietnam/1203/2004 vaccine virus in ferrets. *J Virol* **84**, 6570–6577 (2010). https://doi.org/10.1128/JVI.00221-10
20 Stevens, J. *et al.* Structure and receptor specificity of the hemagglutinin from an H5N1 influenza virus. *Science* **312**, 404–410 (2006). https://doi.org/10.1126/science.1124513
21 Health, E. P. o. A. *et al.* Vaccination of poultry against highly pathogenic avian influenza - Part 2. Surveillance and mitigation measures. *EFSA J* **22**, e8755 (2024). https://doi.org/10.2903/j.efsa.2024.8755
22 Lee, C. W., Senne, D. A. & Suarez, D. L. Effect of vaccine use in the evolution of Mexican lineage H5N2 avian influenza virus. *J Virol* **78**, 8372–8381 (2004). https://doi.org/10.1128/JVI.78.15.8372-8381.2004
23 Yang, Z. Y. *et al.* Immunization by avian H5 influenza hemagglutinin mutants with altered receptor binding specificity. *Science* **317**, 825–828 (2007). https://doi.org/10.1126/science.1135165

24 Chang, P. *et al.* Characterization of the haemagglutinin properties of the H5N1 avian influenza virus that caused human infections in Cambodia. *Emerg Microbes Infect* **12**, 2244091 (2023). https://doi.org/10.1080/22221751.2023.2244091

25 Xiong, X. *et al.* Receptor binding by an H7N9 influenza virus from humans. *Nature* **499**, 496–499 (2013). https://doi.org/10.1038/nature12372

26 Peacock, T. P. *et al.* Variability in H9N2 haemagglutinin receptor-binding preference and the pH of fusion. *Emerg Microbes Infect* **6**, e11 (2017). https://doi.org/10.1038/emi.2016.139

27 Watanabe, Y. *et al.* Acquisition of human-type receptor binding specificity by new H5N1 influenza virus sublineages during their emergence in birds in Egypt. *PLoS Pathog* **7**, e1002068 (2011). https://doi.org/10.1371/journal.ppat.1002068

28 Hensley, S. E. *et al.* Hemagglutinin receptor binding avidity drives influenza A virus antigenic drift. *Science* **326**, 734–736 (2009). https://doi.org/10.1126/science.1178258

29 Peacock, T. P. *et al.* Genetic determinants of receptor-binding preference and zoonotic potential of H9N2 avian influenza viruses. *Journal of Virology* **95**, 10.1128/jvi. 01651–01620 (2021). https://doi.org/https://doi.org/10.1128/jvi.01651-20

30 Medeiros, R., Escriou, N., Naffakh, N., Manuguerra, J. C. & van der Werf, S. Hemagglutinin residues of recent human A(H3N2) influenza viruses that contribute to the inability to agglutinate chicken erythrocytes. *Virology* **289**, 74–85 (2001). https://doi.org/10.1006/viro.2001.1121

31 Heaton, B. E. *et al.* A CRISPR Activation Screen Identifies a Pan-avian Influenza Virus Inhibitory Host Factor. *Cell Rep* **20**, 1503–1512 (2017). https://doi.org/10.1016/j.celrep.2017.07.060

32 Wong, H. H., Fung, K. & Nicholls, J. M. MDCK-B4GalNT2 cells disclose a alpha2,3-sialic acid requirement for the 2009 pandemic H1N1 A/California/04/2009 and NA aid entry of A/WSN/33. *Emerg Microbes Infect* **8**, 1428–1437 (2019). https://doi.org/10.1080/22221751.2019.1665971

33 Linster, M. *et al.* Identification, characterization, and natural selection of mutations driving airborne transmission of A/H5N1 virus. *Cell* **157**, 329–339 (2014). https://doi.org/10.1016/j.cell.2014.02.040

34 Herfst, S. *et al.* Airborne transmission of influenza A/H5N1 virus between ferrets. *Science* **336**, 1534–1541 (2012). https://doi.org/10.1126/science.1213362

35 Matrosovich, M. *et al.* Early alterations of the receptor-binding properties of H1, H2, and H3 avian influenza virus hemagglutinins after their introduction into mammals. *J Virol* **74**, 8502–8512 (2000). https://doi.org/10.1128/jvi.74.18.8502-8512.2000

36 Liu, J. *et al.* Structures of receptor complexes formed by hemagglutinins from the Asian Influenza pandemic of 1957. *Proc Natl Acad Sci U S A* **106**, 17175–17180 (2009). https://doi.org/10.1073/pnas.0906849106

37 Zhang, Y. *et al.* Key Amino Acid Residues That Determine the Antigenic Properties of Highly Pathogenic H5 Influenza Viruses Bearing the Clade 2.3.4.4 Hemagglutinin Gene. *Viruses* **15** (2023). https://doi.org/10.3390/v15112249

38 Davila, K. S. *et al.* Inoculation with highly pathogenic avian influenza H5N1 genotype D1. 1 in naïve dairy cows and dairy cows previously exposed to genotype B3. 13. *Research Square* (2025). https://doi.org/https://doi.org/10.21203/rs.3.rs-8339573/v1

39 Billington, E. *et al.* Investigating factors driving shifts in subtype dominance within H5Nx clade 2.3.4.4b high pathogenicity avian influenza viruses. *J Gen Virol* **106** (2025). https://doi.org/10.1099/jgv.0.002150

40 Zhu, R. *et al.* HA gene amino acid mutations contribute to antigenic variation and immune escape of H9N2 influenza virus. *Vet Res* **53**, 43 (2022). https://doi.org/10.1186/s13567-022-01058-5

41 Sealy, J. E. *et al.* Association of Increased Receptor-Binding Avidity of Influenza A(H9N2) Viruses with Escape from Antibody-Based Immunity and Enhanced Zoonotic Potential. *Emerg Infect Dis* **25**, 63–72 (2018). https://doi.org/10.3201/eid2501.180616

42 Russell, C. J., Hu, M. & Okda, F. A. Influenza Hemagglutinin Protein Stability, Activation, and Pandemic Risk. *Trends Microbiol* **26**, 841–853 (2018). https://doi.org/10.1016/j.tim.2018.03.005

43 Yang, J. *et al.* Emerging Haemagglutinin Mutations in Bovine-origin H5N1 Influenza Viruses from Humans and Cattle Retain Avian Receptor Binding with Increased Stability. *bioRxiv*, 2026.2008. 2018.745528 (2026). https://doi.org/https://doi.org/10.64898/2026.08.18.745528

44 Sukhova, K. *et al.* Mutations in severe human H5N1 cases facilitate evasion from human mucus and antivirals. *bioRxiv*, 2026.2007. 2028.740943 (2026). https://doi.org/https://doi.org/10.64898/2026.07.28.740943

45 Shu, Y. & McCauley, J. GISAID: Global initiative on sharing all influenza data - from vision to reality. *Euro Surveill* **22** (2017). https://doi.org/https://doi.org/10.2807/1560-7917.ES.2017.22.13.30494

46 Neumann, G. *et al.* Generation of influenza A viruses entirely from cloned cDNAs. *Proc Natl Acad Sci U S A* **96**, 9345–9350 (1999). https://doi.org/10.1073/pnas.96.16.9345

47 Elderfield, R. A. *et al.* Accumulation of human-adapting mutations during circulation of A(H1N1)pdm09 influenza virus in humans in the United Kingdom. *J Virol* **88**, 13269–13283 (2014). https://doi.org/10.1128/JVI.01636-14

48 Chang, P., Sealy, J. E., Sadeyen, J. R. & Iqbal, M. Amino Acid Residue 217 in the Hemagglutinin Glycoprotein Is a Key Mediator of Avian Influenza H7N9 Virus Antigenicity. *J Virol* **93** (2019). https://doi.org/10.1128/JVI.01627-18

49 Lin, Y. P. *et al.* Evolution of the receptor binding properties of the influenza A(H3N2) hemagglutinin. *Proc Natl Acad Sci U S A* **109**, 21474–21479 (2012). https://doi.org/10.1073/pnas.1218841110

50 Xiong, X. *et al.* Receptor binding by a ferret-transmissible H5 avian influenza virus. *Nature* **497**, 392–396 (2013). https://doi.org/10.1038/nature12144

51 James, J. *et al.* Clade 2.3.4.4b H5N1 high pathogenicity avian influenza virus (HPAIV) from the 2021/22 epizootic is highly duck adapted and poorly adapted to chickens. *J Gen Virol* **104** (2023). https://doi.org/10.1099/jgv.0.001852

52 Sealy, J. E. *et al.* Adsorptive mutation and N-linked glycosylation modulate influenza virus antigenicity and fitness. *Emerg Microbes Infect* **9**, 2622–2631 (2020). https://doi.org/10.1080/22221751.2020.1850180

53 Chapter, W. 3.3. 4 Avian Influenza (Including Infection with High Pathogenicity Avian Influenza Viruses). *Manual of diagnostic tests and vaccines for terrestrial animals*, 26 (2021).

54 Dholakia, V. *et al.* Polymerase mutations underlie early adaptation of H5N1 influenza virus to dairy cattle and other mammals. *Nat Commun* (2026). https://doi.org/10.1038/s41467-026-68306-6

55 Chang, P. *et al.* Immune Escape Adaptive Mutations in the H7N9 Avian Influenza Hemagglutinin Protein Increase Virus Replication Fitness and Decrease Pandemic Potential. *J Virol* **94** (2020). https://doi.org/10.1128/JVI.00216-20

56 Bordes, L. *et al.* Highly Pathogenic Avian Influenza H5N1 Virus Infections in Wild Red Foxes (Vulpes vulpes) Show Neurotropism and Adaptive Virus Mutations. *Microbiol Spectr* **11**, e0286722 (2023). https://doi.org/10.1128/spectrum.02867-22

57 Klim, H. *et al.* Serological analysis in humans in Malaysian Borneo suggests prior exposure to H5 avian influenza near migratory shorebird habitats. *Nat Commun* **15**, 8863 (2024). https://doi.org/10.1038/s41467-024-53058-y

58 Nagy, A. *et al.* A universal RT-qPCR assay for "One Health" detection of influenza A viruses. *PLoS One* **16**, e0244669 (2021). https://doi.org/10.1371/journal.pone.0244669

59 James, J. *et al.* Rapid and sensitive detection of high pathogenicity Eurasian clade 2.3.4.4b avian influenza viruses in wild birds and poultry. *J Virol Methods* **301**, 114454 (2022). https://doi.org/10.1016/j.jviromet.2022.114454

60 Meng, E. C. *et al.* UCSF ChimeraX: Tools for structure building and analysis. *Protein Sci* **32**, e4792 (2023). https://doi.org/10.1002/pro.4792
61 Katoh, K. & Standley, D. M. MAFFT multiple sequence alignment software version 7: improvements in performance and usability. *Mol Biol Evol* **30**, 772–780 (2013). https://doi.org/10.1093/molbev/mst010
62 Lemey, P., Minin, V. N., Bielejec, F., Kosakovsky Pond, S. L. & Suchard, M. A. A counting renaissance: combining stochastic mapping and empirical Bayes to quickly detect amino acid sites under positive selection. *Bioinformatics* **28**, 3248–3256 (2012). https://doi.org/10.1093/bioinformatics/bts580
63 Suchard, M. A. *et al.* Bayesian phylogenetic and phylodynamic data integration using BEAST 1.10. *Virus Evol* **4**, vey016 (2018). https://doi.org/10.1093/ve/vey016
64 Meredith, M. & Kruschke, J. HDInterval: highest (posterior) density intervals. *CRAN: Contributed Packages* (2016). https://doi.org/10.32614/cran.package.hdinterval
65 R Core Team, R. R: A language and environment for statistical computing. [Internet]. (2024). https://doi.org/https://www.r-project.org/
66 Xu, S. *et al.* Ggtree: A serialized data object for visualization of a phylogenetic tree and annotation data. *Imeta* **1**, e56 (2022). https://doi.org/10.1002/imt2.56
67 Price, M. N., Dehal, P. S. & Arkin, A. P. FastTree: computing large minimum evolution trees with profiles instead of a distance matrix. *Mol Biol Evol* **26**, 1641–1650 (2009). https://doi.org/10.1093/molbev/msp077
68 Tavaré, S. In the analysis of DNA sequences. *Some mathematical questions in biology: DNA sequence analysis* **17**, 57 (1986).

Supplementary Files

This is a list of supplementary files associated with this preprint. Click to download.

- SupplementaryfiguresandtablesH5HAE185K16Oct2026.pdf